THE IMPACT OF HELD AUSTENITE ON THE WEAR COMPONENT OF BAINITIC BENDABLE IRON UNDER SWAY LOAD WARM CONDUCTION

*T.Vinithra Banu, Rajmohan.B**, T.Punitha***
Assistant Professor, Department of Mechanical Engineering
*Prince Shri Venkateshwara Padmavathy Engineering College,Chennai.
**Prince Dr.K.Vasudevan College of Engineering & Technology, Chennai.
***Faculty, Prince Shri Venkateshwara Arts and Science College, Gowriwakkam.

ABSTRACT:
The impact of held austenite on the effect wear opposition of bainitic malleable iron is considered. Two sorts of bainitic malleable iron with various morphologies of held austenite were manufactured through consistent cooling measure. The effect wear test was conveyed out on an effect rough wear analyzer under various burdens. The outcomes showed that the wear conduct of bainitic malleable iron could be partitioned into three phases during the effect wear test. There was a cozy connection between the wear opposition and microstructure portrayal, particularly the morphology, conveyance and security of held austenite. Slender film held austenite with suitable security could improve the wear obstruction of malleable iron, while an enormous number of low solidness and cumbersome held austenite would diminish the wear obstruction under high effect load condition. The wear mass loss of bainitic malleable iron with slender film held austenite (BDI A) was lower than that of bainitic malleable iron with cumbersome held austenite (BDI B). The wear instrument of BDI An is fundamentally furrow wear and exhaustion wear, while that of BDI B is furrow wear, weariness wear and distortion exhaustion chip.

Keywords: Bainitic ductile iron, Retained austenite, Wear mechanism, Impact load

1. Introduction

In recent years, bainitic ductile iron has been widely used in many industrial aspects due to its excellent fatigue strength, high tensile strength, good ductility, and especially great wear resistance [1e4]. Many bainitic ductile iron components such as grinding ball, railway track and gears are performed under impact load condition. The repeated impact load may result in durability loss of a mechanical system and increase the complexity of wear behavior [5]. The mechanical properties of bainitic ductile iron are significantly depended on the microstructure, which mainly consists of bainite, retained austenite, and graphite. For the ductile iron, different microstructure characterization can be obtained by tailoring the alloying composition or heat treatments like aus tempering and continuous cooling [6]. A great number of researches on the wear resistance of bainitic ductile iron have been conducted to investigate the effect of microstructure [7-9]. Zhou et al. [10] found that the performance of the bainite/ martensite ductile iron under the impact wear condition is similar with the high chrome cast iron. Wen et al. [11] have studied the role of two kinds of bainite in the process of friction and wear behavior. The result demonstrated that the wear mechanism belonged to abrasive wear and fatigue delamination fracture, which were mostly decided by the loading state. Sun et al. [12] investigated the dry impact wear behavior of bainitic ductile cast iron. Their study showed that the grain refinement of lower bainite could lead to

excellent mechanical properties including high wear resistance. Sahin et al. [13] examined the abrasive wear of bainite/ferrite dual phase ductile iron. The specimens with dual matrix structure had greater ductility than the traditional aus tempered one. Overall, hardness and impact toughness are the two key factors affecting the wear resistance. For bainitic ductile iron, retained austenite acts as a role balancing the strength and toughness. In mechanical tests, stress and strain induced austenite to martensite transformation have been observed. Zhang et al. [14] found that the subsurface hardness increased because of work hardening and the transformation of retained austenite to martensite. The volume fraction, grain size and morphology will affect the stability of retained austenite [15]. The impact load condition accelerates the strain induced transformation. The relationship between the mechanical stability of retained austenite and wear resistance needs to be clarified. In this study, two kinds of bainitic ductile iron with thin film or bulky retained austenite were obtained. The effect of retained austenite especially the morphology on the wear mechanism of bainitic ductile iron under impact load was studied.

2. Experimental procedures

2.1. Experimental material

In this work, a self-developed bainitic ductile iron is used and the chemical composition is given in Table 1. The raw material powders were provided by the Grinm Advanced Materials Co., Ltd. The experimental material was produced by induction melting and casted into ball of F100 mm in the metal mould. The samples for heat treatment were cut form the as-cast ball. Here continuous cooling process was chosen as the heat treatment procedure. Fig. 1a shows the schematic diagram of heat treatment processes. Some samples were austenitized at 920°C for 2 h, while others were heated at 960°C for 2 h. Both of them were quenched by NaCl solution at ambient temperature and then tempered at 200°C for 2 h followed by air cooling. These two kinds of samples were recorded as BDI A (austenitized at 920°C and tempered at 200°C) and BDI B (austenitized at 960°C and tempered at 200°C), respectively.

2.2. Impact wear test

The impact wear test was carried out on a MLD-10 impact abrasive wear tester with a rotation speed of 100 r/min and at an impact angle of 90° as shown in Fig. 1b. The friction wheel was made of GB: 45 steel and the abrasive particles are quartz sands with particle size of 2.0~4.0 mm. The samples, having a dimension of 10*10*35 mm, were cut from the heat-treated samples (both BDI A and BDI B). The quartz sand particles flew over the surface of the samples in the sliding process with impacting effect. The impact energy for wear test was 1.0, 2.0 and 4.0 J, respectively. The impact frequency was 200 times/min. The weight loss was measured every 3,000 cycles. Under the given impact load, the duration of the whole test was 150 min and 30,000 cycles in total were carried out for each sample. The weight loss was measured using an analytical balance with accuracy of 0.01 mg. The average mass loss was obtained by three parallel experiments.

Table 1 – Chemical composition of the studied ductile iron (wt. %).

C	Si	Mn	V	Cr	Mg	RE	P	S	Fe
3.0	3.8	2.0	0.9	0.2	0.035	0.038	0.016	0.0041	Bal

2.3. Microstructure analysis and mechanical properties test

The samples before and after wear tests were polished and etched with 4 vol% Nital solution. Microstructure analyses were carried out by ZEISS Imager. M2m optical microscope (OM), Zeiss Merlin Compact field emission scanning electron microscope (FE-SEM). JEM-2100 transmission electron microscope (TEM) was also used to observe the microstructure. TEM specimens were grinded to a thickness of 50 mm and electropolished with a twin jet electro polisher (MTP-1A) at 30°C using a solution containing 95 vol% C2H5OH and 5 vol% HClO4.

The volume fraction of retained austinite was obtained by Xray diffraction (XRD: Rigaku Smart Lab, Cu target, operated at 40 kV and 150 mA with scanning speed 20_/min) analysis. The volume fraction was determined by comparison method using the integrated intensities of {200}, {220}, {311} austenitic peaks and {200}, {211} ferritic peaks according to the standard of YB/ T5338-2006. The hardness and impact toughness were measured using a TH320 Rockwell hardness tester and TB300 impact machine, respectively. FE-SEM was used to analyze the morphological features of wear surface and the cross section of samples.

3. Results and discussion

3.1. Microstructure characterization and mechanical properties

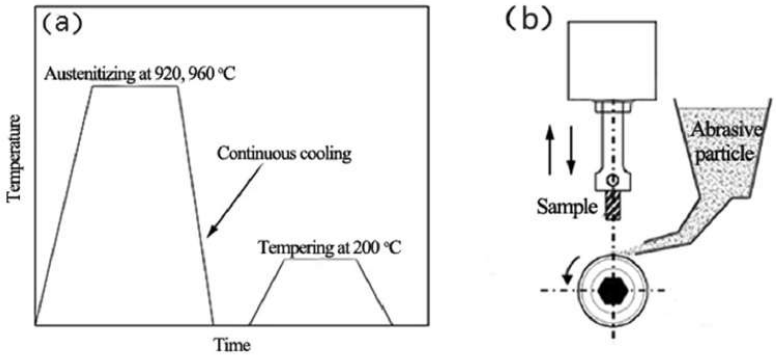

Fig. 1 – (a) Schematic diagram of continuous cooling process; (b) Schematic diagram of MLD-10 impact abrasive wear tester.

Fig. 2 shows the microstructure of samples austenitized at 920°C (BDI A) and 960°C (BDI B), respectively. Both microstructures consist mainly of graphite, bainite and retained austenite. No ferrite could be observed after quenching and tempering. More austenite is retained for BDI B as shown in Fig. 2b and it can be confirmed by the XRD curves in Fig. 3. The volume fraction of retained austenite for BDI B is about 15.4%. The higher austenitizing temperature increases the austenite stability and more austenite is retained after quenching [17,18]. However, the morphology of retained austenite is totally different. Bulky retained austenite accumulates near the graphite and evolves into a C-area for BDI B [19]. The grain

size of bulky retained austenite falls between 10~20 mm range. But the retained austenite is not obvious for BDI A in the OM image of Fig. 2a. Fig. 2c shows that austenite and bainite exist alternatively for BDI A and the retained austenite demonstrates thin film shape. When the austenitizing temperature increases from 920 _C to 960 _C, the graphite becomes smaller due to dissolution and some small graphite even disappears. Thus the carbon content near the graphite increases and large amount of bulky austenite is retained after continuous cooling. The hardness value for BDI A and BDI B both falls into 51~53 HRC and no obvious difference is found. The impact hardness for BDI A is 16.1 J_cm_2, which is higher than that for BDI B with 13 J_cm_2 (Table 2). The relationship between initial microstructure and mechanical properties with the impact wear behavior will be discussed in the following section.

3.2. Wear behavior

Fig. 4 shows the changes of wear mass loss with time under different impact loads. The evolution of wear mass loss is closely related with the impact time, load and initial microstructure.

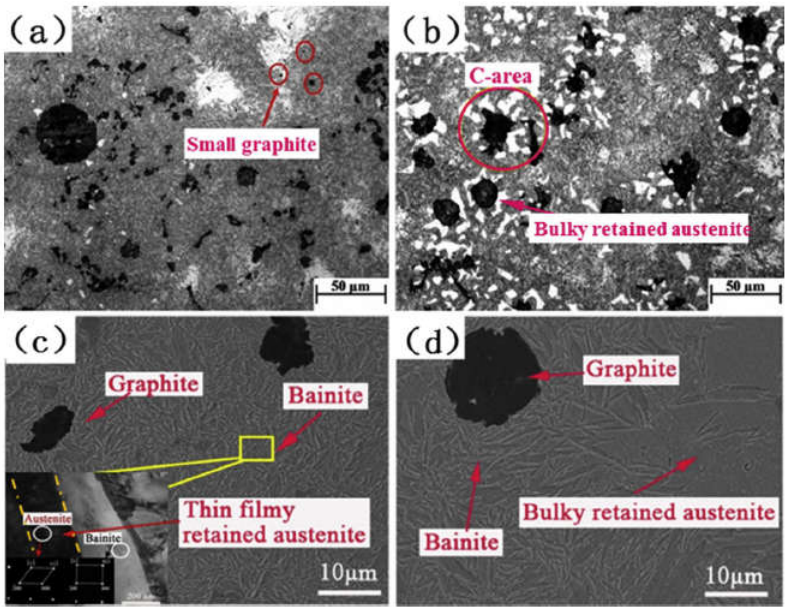

Fig. 2 – Microstructure at the initial state. OM image of (a) BDI A and (b) BDI B; SEM secondary electron (SE) image of (c) BDI A (the inset shows TEM micrograph and selected area diffraction pattern (SADP) of austenite and bainite and the white circles indicate areas from where SADP were taken) and (d) BDI B.

As shown in Fig. 4a, the weight loss is similar at the initial stage. The weight loss remains increasing with the process of wear test. But the weight loss gap becomes large among different samples. It should be noted that the change of wear mass loss for BDI B under 4 J impact load is quite different from other conditions, which indicates that the wear behavior is changed especially near the end of the wear test. Fig. 4b shows the relationship between the accumulative wear mass loss and impact load of the two samples after 30,000 cycles. As the impact load increases, the wear mass loss of BDI A gradually decreases, while the wear mass loss of BDI B climbs sharply form 0.45-0.87 g. Under the same experimental condition, the wear resistance of BDI A is better than BDI B, and this behavior is gradually strengthened

with the increase of impact load. When the impact load is 4 J, the wear mass loss of BDI B is about four times as much as BDI A. It is known that impact load plays two vital roles during the wear process. On the one hand, the increase of impact load results in the sharp increase of friction between the sample and abrasive particles, thus improving the wear rate [20]. On the other hand, the increase of impact load can effectively promote the strain hardening and then help increase the wear resistance [21-23]. For BDI A, the latter one might be the crucial role.
To investigate the wear behavior from amore precise view, the wear rate variation of different samples with time is calculated according to the wear mass loss data. As shown in Fig. 5, the wear process of the two kinds of samples can be both divided into three stages. Stage 1 is the initial stage of wear. The surface of the sample and the friction wheel are rough and an unsmooth interface exists. When relative motion occurs between the sample and friction wheel, the asperities on the surface are worn flat and the wear rate increases slowly. As the wear test continues running, the wear behavior steps into the next stage. Stage 2 is the stable wear stage in which the wear rate decreases slightly and tends to be stable. Finally, stage 3 is the stage of severe wear where fatigue occurs on the worn surface and the wear rate increases. Initially, the wear is relatively easy due to the rough surface and unsmooth interface. For the transition of wear rate, it should be noted that a large number of dislocations are generated on the surface of the sample under the repeated impact load, which leads to strain hardening. Strain induced phase transformation from retained austenite to martensite maybe process during plastic deformation [24]. This can be proved by the XRD patterns of BDI A and BDI B before and after the wear test shown in Fig. 6. Finally, the contact area between the samples and friction wheel increases, leading to the reduction of contact stress. These factors lead to the transition of wear rate in stage 2.

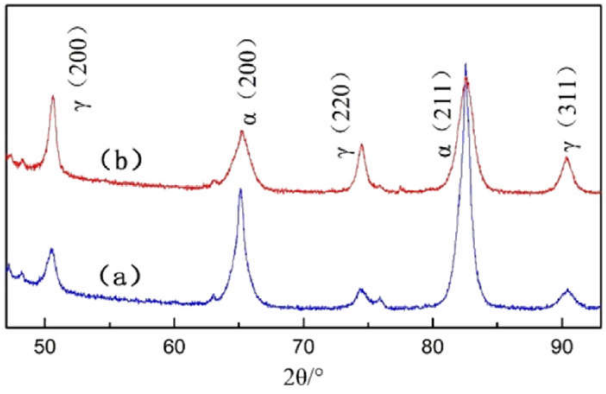

Fig. 3 – XRD curves of ductile irons for the BDI A (a) and BDI B (b).

For BDI A, the wear rate decreases gradually with the increase of impact load as shown in Fig. 4b. The increase of the impact load may lead to more fierce friction and then increase the wear rate. But high impact load can also contribute to the strain hardening of the sample and then help increase the wear resistance. Zorgani et al. [25] proposed that the stability of retained austenite was a function of percent deformation. The martensite transformation will be induced in the matrix with the increase of impact load. The alternative bainite and austenite laths lead to appropriate stability of the retained austenite film [15]. The martensite with high hardness is distributed in the matrix of high strength bainite with certain toughness,

which significantly strengthens the surface of the sample. The abrasive particles are hard to extrude into the hard surface and the wear resistance is improved. While for BDI B, the wear rate increases dramatically, even jumping to 6.0 _ 10_3 from 0.9 _ 10_3 g/min. This is mainly due to that the stability of bulky retained austenite is low and the martensite transformation is easy to be induced. The peak g(220) of austenite is invisible for BDI B under 4 J impact load. The sample with coarse bulky and brittle martensite is prone to cause brittle delamination in the process of high impact energy, which greatly accelerates the wear rate. The cross section of samples after impact wear test also shows similar results that the wear resistance of BDI A is better than that of BDI B. For BDI A, the morphology of graphite at the subsurface is similar with the initial state before wear test. Rare cracks could be observed. But the graphite is deformed severely for BDI B and many cracks and delamination could be seen in Fig. 7b. The result indicates the poor deformation behavior of matrix brittle bulky martensite.

Table 2 – Summary of characterization for the ductile irons.

Sample	Volume fraction of bainite/%	Volume fraction of graphite/%	Volume fraction of retained austenite/%	Carbon content of retained austenite/wt%	Rockwell hardness/ HRC	Impact toughness/ $J \cdot cm^{-2}$
BDI A	87.1 ± 1.2	4.3 ± 0.8	8.6 ± 0.7	1.15 ± 0.2	51.5 ± 0.6	16.1 ± 0.9
BDI B	79.9 ± 1.5	3.7 ± 0.6	15.4 ± 0.9	2.02 ± 0.3	53.0 ± 0.9	13 ± 1.0

3.3. Worn surface and wear mechanism

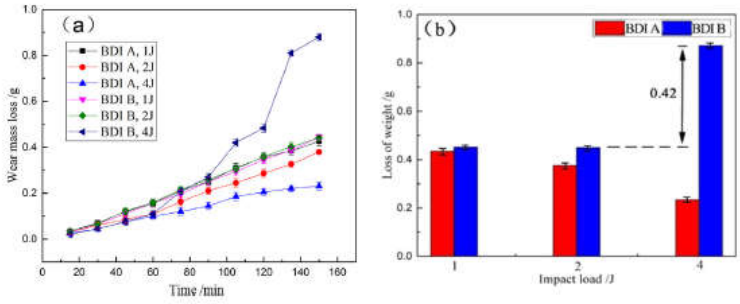

Fig. 4 – Wear mass loss with time (a) and total weight loss (b) of the samples under different load conditions.

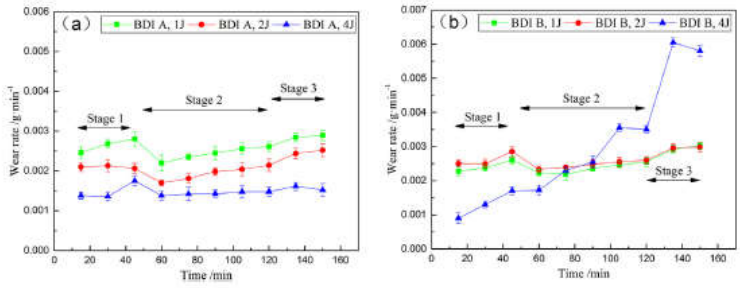

Fig. 5 – Wear rate variation of different samples with time: (a) BDI A; (b) BDI B.

The worn surfaces of BDI A and BDI B after impact wear test are shown in Fig. 8 and Fig. 9, respectively. In the process of impact wear, abrasive particles are flowing between the sample and friction wheel, and the former impacts the latter periodically. For BDI A, it demonstrates high strength and enough toughness due to the existence of a thin film associated with retained austenite-bainite structure. No obvious impact pits can be seen on the worn surface, and the surface is relatively flat after low impact load as shown in Fig. 8a. Under high contact

pressure, materials exchange occurs frequently between the abrasive particles and the sample. Meanwhile, the abrasive particles will be squeezed into the surface of the sample and thus the furrow will be generated. The strong shear and tensile stress promote the initiation and propagation of microcracks on the worn surface [26]. In addition, the fatigue wear is observed as shown in Fig. 8b. Therefore, the wear mechanism of BDI A is mainly plough wear and fatigue wear.

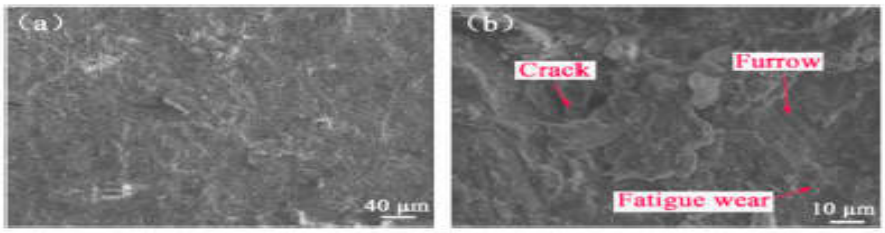

Fig. 8 – Observation of worn surface of BDI A after impact wear: (a) 1 J; (b) 4 J.

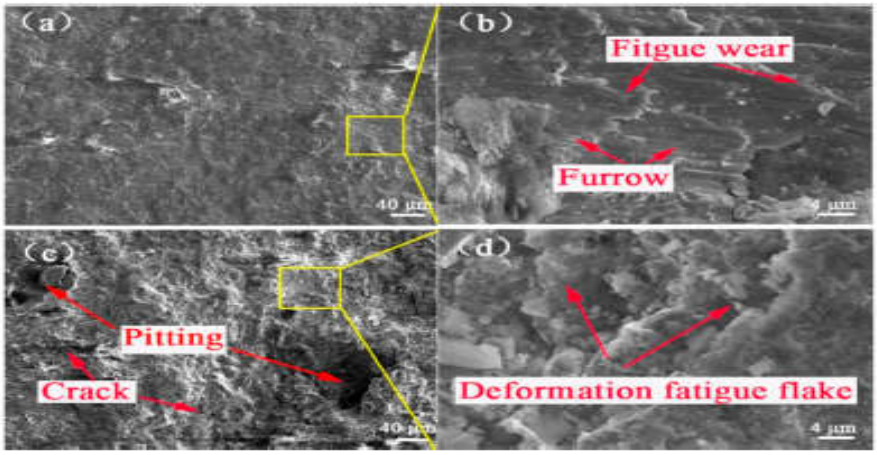

Fig. 9 – Observation of worn surface of BDI B after impact wear under (a, b) 1J and (c, d) 4J impact load.

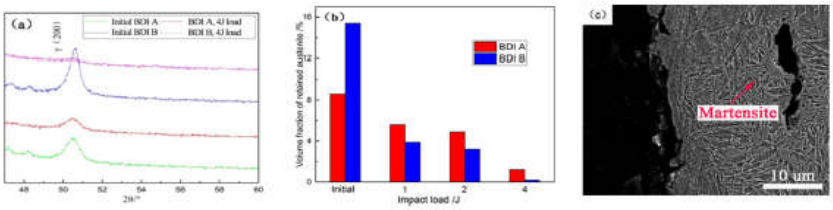

Fig. 6 – XRD curves for samples before and after wear test (a); volume fraction of retained austenite of different samples (b); microstructure of BDI B after wear test at 4 J (c).

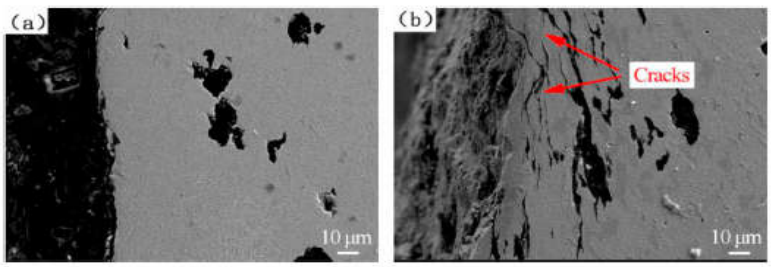

Fig. 7 – The cross section of samples after impact wear test under 4 J: (a) BDI A; (b) BDI B.

In case of BDI B, the worn surface and wear mechanism is similar with that of BDI A when the impact load is low (1 J). However, when the impact load climbs up to 4 J, the wear phenomenon changes dramatically. First, big impact pits and cracks appear on the worn surface, as shown in Fig. 9c. Fig. 9d indicates that a large amount of plastic deformation takes place due to the transformation from bulky austenite into coarse and brittle martensite. The surface of sample continues to be peeled off. In addition, the wear mass loss increases sharply after 90 min wearing as shown in Fig. 5b. Consequently, the main wear mechanism of BDI B is plough wear at the beginning and deformation fatigue flake at the end under high impact load condition.

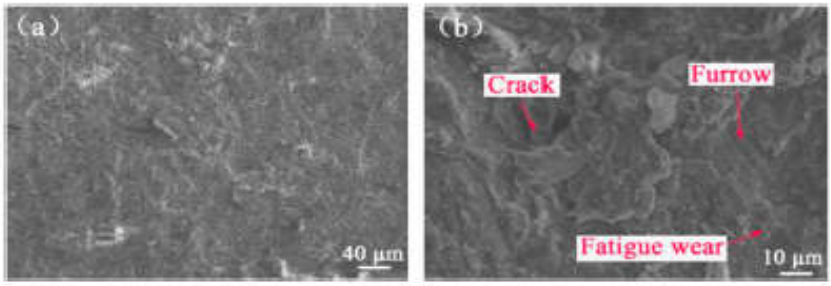

Fig. 8 – Observation of worn surface of BDI A after impact wear: (a) 1 J; (b) 4 J.

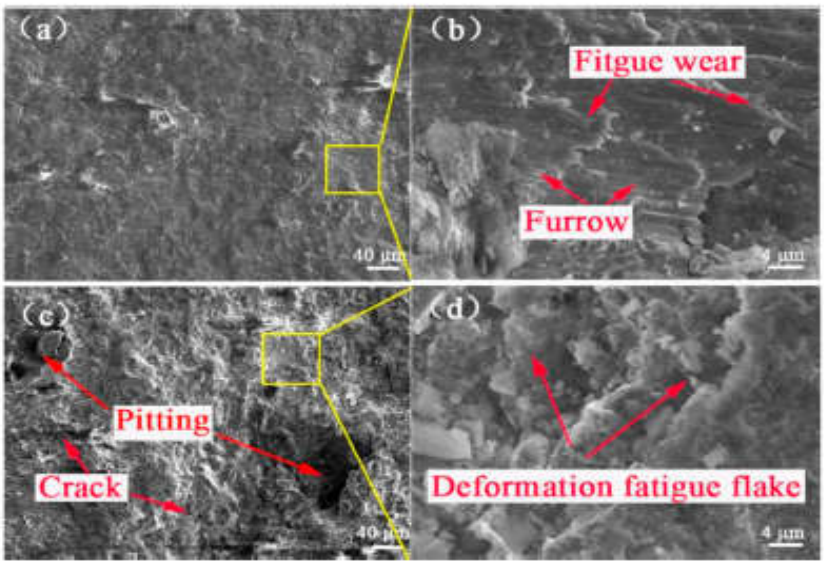

Fig. 9 – Observation of worn surface of BDI B after impact wear under (a, b) 1J and (c, d) 4J impact load.

4. Conclusions

The effect of retained austenite on the impact wear resistance of bainitic ductile iron is studied. The results show that there is a close relationship between the wear resistance and the morphology of retained austenite. The following conclusions are drawn:

The wear behavior of bainitic ductile iron could be divided into three stages during the impact wear test. At the initial stage 1, the wear is relatively easy due to the rough surface

and unsmooth interface. As the wear test continues running, the wear rate decreases slightly and tends to be stable. Obvious strain hardening and strain induced martensite transformation is activated, which significantly improves the wear resistance in stage 2. Fatigue occurs on the worn surface and the wear rate increases at the final stage 3.

The microstructure characterization of the bainitic ductile iron, especially the morphology, distribution and stability of retained austenite has a strong influence on the wear resistance. Thin film retained austenite with appropriate stability can improve the wear resistance of ductile iron, while a large number of low stability and bulky retained austenite will dramatically reduce the wear resistance in the process of high impact load condition.

The wear mass loss of BDIA with thin film retained austenite is lower than that of BDI B with bulky retained austenite under different impact loads. The wear mechanism of BDI A is mainly plough wear and fatigue wear, while that of BDI B is plough wear, fatigue wear and deformation fatigue flake.

References

[1] Panneerselvam S, Putatunda SK, Gundlach R, Boileau J. Influence of intercritical austempering on the microstructure and mechanical properties of austempered ductile cast iron (ADI). Mater Sci Eng A 2007;694:72e80.

[2] _Soli_c S, Godec M, Schauperl Z, Donik _C. Improvement in abrasion wear resistance and microstructural changes with deep cryogenic treatment of austempered ductile cast iron (ADI). Metall Mater Trans A 2006;47:5058e70.

[3] Basso A, Sikora MJ. Influence of section size on dual phase ADI microstructure and properties: comparison with fully ferritic and fully aus ferritic matrices. Mater Sci Technol 2009;25:1271e8.

[4] Cui J, Chen L. Microstructure and abrasive wear resistance of an alloyed ductile iron subjected to deep cryogenic and austempering treatments. Mater Sci Technol 2011;12:1549e54.

[5] Yilmaz H, Sadeler R. Impact wear behavior of ball burnished 316L stainless steel. Surf Coat Technol 2009;363:369e78.

[6] Soliman M, Ibrahim H, Nofal A, Palkowski H. Thermo mechanically
processed dual matrix ductile iron produced by continuous cooling transformation. J Mater Process Technol 2006;227:1e10.

[7] Sinlah A, Handayani D, Voigt RC, Hayrynen K, M'Saoubi R, Saldana C. Effects of microstructure and strength on wear performance in rough milling of austempered ductile iron. Int J Cast Met Res 2006;29:62e7.

[8] Lefevre J, Hayrynen KL. Austempered materials for powertrain applications. J Mater Eng Perform 2013;22:1914e22.

[9] Martins R, Seabra J, Magalh~aes L. Austempered ductile iron (ADI) gears: power loss, pitting and micropitting. Wear 2008;264:838e49.

[10] Zhou R, Jiang Y, Lu D, Zhou R, Li Z. Development and characterization of a wear resistant bainite/martensite ductile iron by combination of alloying and a controlled cooling heat-treatment. Wear 2001;250:529e34.

[11] Wen F, Zhao J, Zheng D, He K, Ye W, Qu S, et al. The role of bainite in wear and friction behavior of austempered ductile iron. Materials 2011;12:767e79.
[12] Sun T, Song R, Yang F, Wu C. Wear behavior of bainite ductile cast iron under impact load. Int J Miner Metall Mater 2014;21:871e7.
[13] Sahin Y, Kilicli V, Ozer M, Erdogan M. Comparison of abrasive wear behavior of ductile iron with different dual matrix structures. Wear 2010;268:153e65.
[14] Zhang N, Zhang J, Lu L, Zhang M, Zeng D, Song Q. Wear and friction behavior of austempered ductile iron as railway wheel material. Mater Des 2016;89:815e22.
[15] Gao G, Liu R, Wang K, Gui X, Misra RDK, Bai B. Role of retained austenite with different morphologies on subsurface fatigue crack initiation in advanced bainitic steels. Scripta Mater 2000;184:12e8.
[16] Roberts CS. Effect of carbon on the lattice parameter of austenite. Trans AIME 1982;197:203e4.
[17] Li J, He T, Zhang P, Cheng L, Wang L. Effect of large-size carbides on the anisotropy of mechanical properties in 11Cr- 3Co-3W martensitic heat-resistant steel for turbine high temperature blades in ultra-supercritical power plants. Mater Char 2000;159:110025.
[18] Panneerselvam S, Martis CJ, Putatunda SK, Boileau JM. An investigation on the stability of austenite in austempered ductile cast iron (ADI). Mater Sci Eng A 2015;626:237e46.
[19] Xu Z, Li L. Wear behavior of austenite steel matrix composite reinforced by in situ granular eutectics in impact abrasion. Mater Sci Eng A 2006;428:256e61.
[20] Foglio E, Lusuardi D, Pola A, La Vecchia GM, Gelfi M. Fatigue design of heavy section ductile irons: influence of chunky graphite. Mater Des 2016;111:353e61.
[21] Peng S, Song R, Sun T, Yang F, Deng P, Wu C. Surface failure behavior of 70Mn martensite steel under abrasive impact wear. Wear 2016;362e363:129e34.
[22] Wang B, Barber GC, Qiu F, Zou Q, Yang H. A review: phase transformation and wear mechanisms of single-step and dual-step austempered ductile irons. J Mater Res Technol2002;9:1054e69.
[23] Liu B, Li W, Lu X, Jia X, Jin X. An integrated model of impactabrasive wear in bainitic steels containing retained austenite. Wear 2009;440e441:203088.
[24] Zorgani M, Garcia-Mateo C, Jahazi M. The role of ausforming in the stability of retained austenite in a medium-C carbide-free bainitic steel. J Mater Res Technol2002;9:7762e76.